Diastereoselective Synthesis of Arene Ruthenium(II) Complexes Containing Chiral Phosphetane-Based Tethers[†,1]

Patrícia Pinto,[‡] Andreas W. Götz,[§] Guido Marconi,[‡] Bernd A. Hess,[§,||] Angela Marinetti,[⊥] Frank W. Heinemann,[‡] and Ulrich Zenneck*[,‡]

Institut für Anorganische Chemie, Universität Erlangen-Nürnberg, Egerlandstrasse 1, D-91058 Erlangen, Germany, Institut für Physikalische und Theoretische Chemie, Universität Erlangen-Nürnberg, Egerlandstrasse 3, D-91058 Erlangen, Germany, and Institut de Chimie des Substances Naturelles CNRS, 1, Avenue de la Terrasse, 91189 Gif-sur-Ivette Cedex, France

Received June 7, 2005

Enantiomerically pure cyclic (*R*,*R*)-sulfates have been transformed into novel enantiopure ligands of the general type (*S*,*S*)-2,4-R_2-1-(3-phenylpropyl)phosphetane (**7a**−**c**; R = Cy, *i*-Pr, *t*-Bu). **7a**−**c** split the arene ruthenium complex dimer [{$RuCl_2(\eta^6$-$C_6H_5COOMe)\}_2$] (**8**) by forming the mononuclear σ complexes (S_C,S_C)-[$RuCl_2(\eta^6$-$C_6H_5COOMe)$\{2,4-R_2-1-(3-phenylpropyl)-η^1-phosphetane\}] (**9a**−**c**). An intramolecular arene ligand displacement reaction leads to (S_C,S_C)-[$RuCl_2$\{2,4-R_2-1-(η^6-3-phenylpropyl)-η^1-phosphetane\}] (**10a**−**c**) with tethered side chains of the arene ligand. Nucleophilic substitution of a chloride ligand by aniline with the assistance of $NaPF_6$ gives access to the diastereomeric complex salts (S_C,S_C)-[RuCl(aniline)\{2,4-R_2-1-(η^6-3-phenylpropyl)-η^1-phosphetane\}] (**11a**−**c**). Good diastereoselectivities were obtained with de values between 84 and 88%. The absolute structures of the major diastereomers of **11a**−**c** have been determined by X-ray structure analysis. R_{Ru},S_C,S_C configurations were found in all cases. DFT calculations performed on the dechlorinated 16-valence-electron intermediate cation (S_C,S_C)-[RuCl\{2,4-di-*tert*-butyl-1-(η^6-3-phenylpropyl)-η^1-phosphetane\}]$^+$ ([**12**]$^+$) are in favor of an attack of aniline from the pro-R_{Ru} side of the complex. Investigation of the relative stabilities of the R_{Ru} and S_{Ru} diastereomers of the complex cation [**11c**]$^+$ revealed an almost isoenergetic situation. The diastereoselectivity of the ligand exchange reaction is therefore believed to be kinetically controlled.

Introduction

Enormous progress has been made in the field of asymmetric ruthenium complex chemistry over the past decade.[2−8] One reason for the still increasing interest in this class of compounds is their importance in catalysis. Asymmetric arene ruthenium complexes can, for example, be used in catalytic Diels−Alder reactions,[9] in alkene metathesis,[10] in cyclopropanation,[11] and as enantioselective hydrogen transfer catalysts for carbonyl or imine group reduction.[12,13] In the actual development of effective catalysts for asymmetric synthesis, much attention has been given to the chemistry of tethered arene Ru(II) complexes (η^6:η^1-arene∩donor, where ∩ denotes the link between an arene ring and a σ-donor center). In such complexes, one or more hydrogen atoms of the arene ring are replaced by a side chain, which contains a ligand function in a suitable distance to the ring for complexing the central metal. Tethering the side chain to the metal atom has the following consequences.

(a) The chelate effect stabilizes such complexes toward arene ligand substitution,[14] and that should be true for the species involved in catalytic cycles as well.

(b) In the case of a chiral arene ligand side chain, it connects the stereogenic center of the organic backbone with the ruthenium metal atom by σ bonds and thus causes a highly restricted stereochemical situation in the coordination sphere.

(c) The tether contributes to the symmetry of the piano-stool-structured catalyst by creating diastereomers with a stereogenic metal center, if the two other σ-ligands of the metal are different.

Examples of tethered η^6-arene ruthenium(II) complexes have been reported with nitrogen, oxygen,[15,16] and phosphorus[14,15,17−21] donor atoms.

* To whom correspondence should be addressed: Fax: int. + 49 9131 852 7367. E-mail: Ulrich.Zenneck@chemie.uni-erlangen.de.

† Dedicated to Prof. Rudi van Eldik on the occasion of his 60th birthday.

‡ Institut für Anorganische Chemie, Universität Erlangen-Nürnberg.

§ Deceased.

|| Institut für Physikalische und Theoretische Chemie, Universität Erlangen-Nürnberg.

⊥ Institut de Chimie des Substances Naturelles CNRS.

(1) Chiral Arene Ruthenium Complexes. 7. Part 6: Pinto, P.; Marconi, G.; Heinemann, F. W.; Zenneck, U. *Organometallics* **2004**, *23*, 374.

(2) Brunner, H.; Gastinger, R. G. *J. Organomet. Chem.* **1978**, *145*, 365.

(3) Brunner, H.; Nuber, B.; Prommesberger, M. *Tetrahedron: Asymmetry* **1998**, *9*, 3223.

(4) Pertici, P.; Pitzalis, E.; Marchetti, F.; Rosini, C.; Salvadori, P.; Bennett, M. A. *J. Organomet. Chem.* **1994**, *466*, 221.

(5) Davenport, A. J.; Davies, D. L.; Fawcett, J.; Russell, D. R. *J. Chem. Soc., Perkin Trans. 1* **2001**, 1500.

(6) Therrien, B.; König, A.; Ward, T. R. *Organometallics* **1999**, *18*, 1565.

(7) den Reijer, C. J.; Wörle, M.; Pregosin, P. S. *Organometallics* **2000**, *19*, 309.

(8) Ganter, C. *Chem. Soc. Rev.* **2003**, *32*, 130.

(9) Faller, J. W.; Lavoie, A. *J. Organomet. Chem.* **2001**, *630*, 17.

(10) Dominique, J.; Delaude, L.; Simal, F.; Demonceau, A.; Noels, A. F. *J. Organomet. Chem.* **2001**, *630*, 17.

(11) Lasa, M.; Lopez, P.; Cativiela, C.; Carmona, D.; Oro, L. A. *J. Mol. Catal. A: Chem.* **2005**, *234*, 129.

(12) (a) Haack, K. J.; Hashiguchi, S.; Fujii, A.; Ikariya, T.; Noyori, R. *Angew. Chem., Int. Ed. Engl.* **1997**, *36*, 285; *Angew. Chem.* **1997**, *109*, 297. (b) Noyori, R.; Yamakawa, M.; Hashiguchi, S. *J. Org. Chem.* **2001**, *66*, 7931.

(13) Petra, D. G. I.; Reek, J. N. H.; Handgraaf, J. W.; Meijer, E. J.; Dierkes, P.; Kamer, P. C. J.; Brussee, J.; Schoemaker, H. E.; van Leeuwen, P. W. N. M. *Chem. Eur. J.* **2000**, *6*, 2818.

(14) Smith, P. D.; Wright, A. D. *J. Organomet. Chem.* **1998**, *559*, 141.

(15) Miyaki, Y.; Onishi, T.; Kurosawa, H. *Inorg. Chim. Acta* **2000**, *300*, 369.

(16) Marconi, G.; Baier, H.; Heinemann, F. W.; Pinto, P.; Pritzkow, H.; Zenneck, U. *Inorg. Chim. Acta* **2003**, *352*, 188.

10.1021/om050461z CCC: $33.50
Publication on Web 04/05/2006

Scheme 1

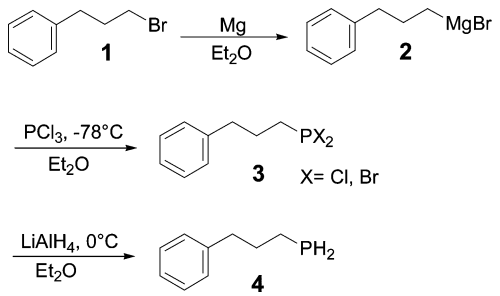

In previous studies we investigated arene ruthenium(II) complexes bearing an enantiopure arene ligand with an OH donor group in the side chain[16] and a series of arene ruthenium(0) complexes with peripheral N or O donors.[22] Enantiopure diphenyl((*R*)-3-phenylbutyl)phosphane as a η^6:η^1-arene∩PPh_2 ligand of Ru(II) finally combines a high diastereoselectivity in σ-ligand exchange reactions and a configurationally stable metal center.[1]

The synthesis of phosphetanes from readily available primary phosphanes and 1,3-diols, as well as their use in asymmetric catalysis, is well-known.[23−28] Due to the low conformational flexibility of the four-membered ring, a positive effect on asymmetric processes is thereby expected.

In this paper we report on the preparation of novel tethered arene ruthenium(II) complexes with enantiomerically pure monodentate phosphetane moieties and their diastereoselective ligand substitution chemistry.

Results and Discussion

Potential tethered η^6:η^1-arene∩phosphetane ruthenium complexes could be prepared from primary phosphanes bearing a phenyl group two or three methylene groups away from the PH_2 terminus. Due to the efficient stereochemical control obtained previously with diphenyl-((*R*)-3-phenylbutyl)phosphane ruthenium complexes,[1] we targeted first a novel arene∩phosphetane ligand with three sp^3 carbon atoms as linkers between the two coordinating sites. The corresponding primary phosphane has been prepared as follows.

Commercially available (3-phenylpropyl)bromide (**1**) can be easily converted into the corresponding Grignard reagent **2,** which was subsequently transformed into the organyl dihalogenophosphane **3** (Scheme 1). Reduction of **3** in ether at 0 °C with $LiAlH_4$ led to the targeted primary phosphane **4**. Workup by vacuum distillation resulted in the isolation of **4** as an air-sensitive, viscous, strongly odorous, and colorless oil.

Scheme 2

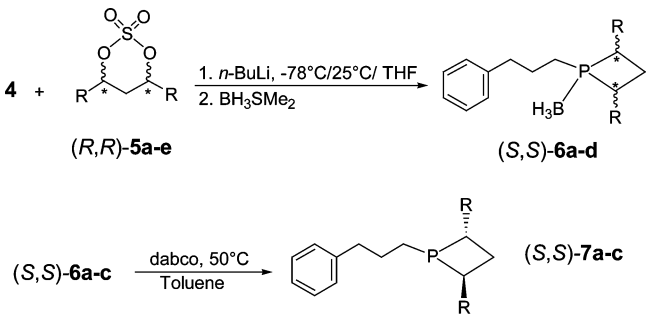

a R=Cy; **b** R=*i*-Pr; **c** R=*t*-Bu; **d** R=Bz; **e** R=Me

Phosphane **4** was reacted with a series of enantiopure cyclic (*R*,*R*)-sulfates (**5a**−**e**),[25,26,29] which were obtained from the corresponding chiral 1,3-diols. Addition of 2.2 equiv of *n*-BuLi at −78 °C in THF gives the respective phosphetanes. A double phosphorus deprotonation is assumed to take place with concomitant addition of the phosphido anion to the cyclic sulfate and final cyclization. Addition of an excess of BH_3·SMe_2 to the reaction mixture led to the isolation of the colorless phosphetane borane complexes **6a**−**d**, which are inert with respect to accidental oxidation during the workup procedures. The adducts **6a** (R = Cy) and **6d** (R = Bz) were isolated as crystalline solids, while **6b** (R = *i*-Pr) and **6c** (R = *t*-Bu) were obtained as oils. Unexpectedly low yields were obtained for **6c**,**d** (20 and 18%, respectively). The attempted reaction of the least sterically hindered cyclic sulfate, **5e** (R = Me), resulted in the formation of a complex mixture of products, which resisted all our efforts to separate it into defined fractions. Probably the methyl substituents supply too little steric protection to allow a straightforward reaction. In the case of the *t*-Bu derivative **5c**, the reaction remained always somewhat incomplete, independently from the reaction time. Some unreacted cyclic sulfate **5c** was always observed together with the product **6c** (Scheme 2).

The molecular structures of **5c** and **6a**,**d** were determined by single-crystal X-ray analysis and are shown in Figures 1−3, respectively. All crystals under study turned out to consist of pure enantiomers, as was evidenced by their chiral space groups and the refinement of the absolute structure parameter. Selected bond distances and angles are given in Table 1, and crystal-

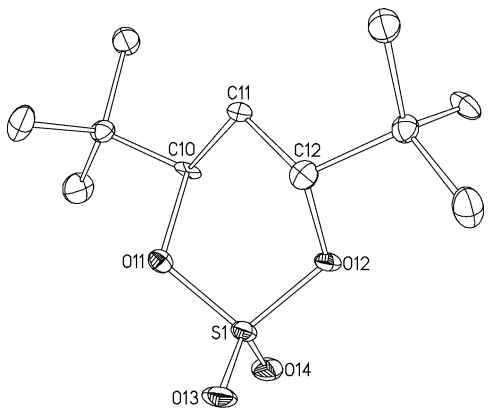

Figure 1. Thermal ellipsoid plot (50% probability) of the molecular structure of the *R*,*R* cyclic sulfate **5c** in the solid state. Hydrogen atoms have been omitted for clarity.

(17) Therrien, B.; Ward, T. R.; Pilkington, M.; Hoffman, C.; Gilardoni, F.; Weber, J. *Organometallics* **1998**, *17*, 330.
(18) Bennett, M. A.; Edwards, A. J.; Harper, J. R.; Khimyak, T.; Willis, A. C. *J. Organomet. Chem.* **2001**, *629*, 7.
(19) Smith, P. D.; Gelbrich, T.; Hursthouse, M. B. *J. Org. Chem.* **2002**, *659*, 1.
(20) Faller, J. W.; D'Alliessi, D. G. *Organometallics* **2003**, *22*, 2749.
(21) Abele, A.; Wursch, R.; Klinga, M.; Rieger, B. *J. Mol. Catal.* **2000**, *160*, 23.
(22) (a) Bodes, G.; Heinemann, F. W.; Marconi, G.; Neumann, S.; Zenneck, U. *J. Organomet. Chem.* **2002**, *641*, 90. (b) Bodes, G.; Heinemann, F. W.; Jobi, G.; Klodwig, J.; Neumann, S.; Zenneck, U. *Eur. J. Inorg. Chem.* **2003**, 281.
(23) Marinetti, A.; Kruger, V.; Buzin, F. X. *Tetrahedron Lett.* **1997**, *17*, 2947.
(24) Marinetti, A.; Kruger, V.; Buzin, F. X. *Coord. Chem. Rev.* **1998**, *178*, 755.
(25) Marinetti, A.; Genêt, J. P.; Jus, S.; Blanc, D.; Ratovelomanana-Vidal, V. *Chem. Eur. J.* **1999**, *5*, 1160.
(26) Marinetti, A.; Jus, S.; Genêt, J. P.; Ricard, L. *Tetrahedron* **2000**, *56*, 95.
(27) Marinetti, A.; Jus, S.; Labrue, F.; Lemarchand, A.; Genêt, J. P.; Ricard, L. *Synthesis* **2001**, *14*, 2095.
(28) Marinetti, A.; Carmichael, D. *Chem. Rev.* **2002**, *102*, 201.

Table 1. Selected Bond Distances (Å) and Angles (deg) for 5c and 6a,d

5c		6a		6d	
		Bond Distances			
S(1)−O(11)	1.565(2)	P(1)−C(9)	1.812(2)	P(1)−C(9)	1.815(3)
S(1)−O(12)	1.566(2)	P(1)−C(10)	1.851(2)	P(1)−C(10)	1.834(3)
S(1)−O(13)	1.425(2)	P(1)−C(12)	1.840(2)	P(1)−C(12)	1.853(3)
S(1)−O(14)	1.424(2)	P(1)−B(1)	1.908(3)	P(1)−B(1)	1.911(4)
C(10)−O(11)	1.498 (4)	C(10)−C(11)	1.574(3)	C(10)−C(11)	1.551(4)
C(10)−C(11)	1.516(4)	C(11)−C(12)	1.560(3)	C(11)−C(12)	1.565(4)
C(11)−C(12)	1.533(4)				
		Bond Angles			
O(13)−S(1)-O(14)	118.6(2)	C(10)−P(1)−C(12)	80.1(2)	C(10)−P(1)−C(12)	79.1(2)
O(11)−S(1)−O(12)	101.5(2)	C(11)−C(10)−P(1)	88.9(2)	C(11)−C(10)−P(1)	87.9(2)
C(10)−C(11)−C(12)	112.0(3)	C(11)−C(12)−P(1)	89.7(2)	C(11)−C(12)−P(1)	86.9(2)
S(1)−O(11)−C(10)	114.8(2)	C(12)−C(11)−C(10)	98.5(2)	C(12)−C(11)−C(10)	97.8(2)

lographic data are given in Table 2. The cyclic sulfate ring of **5c** is strained, as indicated by the intracyclic bond angles, which deviate significantly from their theoretical value of 109.5° for undisturbed sp^3 centers, and exhibits an *R*,*R* configuration of the two stereogenic centers. As observed in the synthesis of related phosphetanes,[25] inversion of the stereochemistry at the carbon centers of **6a**,**d** was found with respect to the corresponding cyclic sulfates. Due to the different covalent radii of phosphorus and carbon atoms, and as usual for this class of compounds, the phosphetane rings form kitelike structures with P−C bonds in the close range of 1.81−1.85 Å and C−C bonds between 1.55 and 1.57 Å. The intracyclic bond angles form a consistent pattern with small C−P−C angles (80.03 and 79.09°,

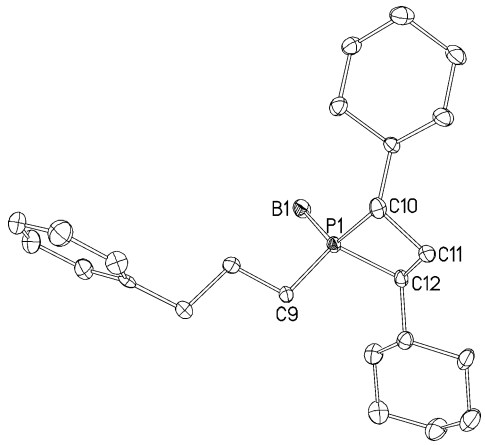

Figure 2. Thermal ellipsoid plot (50% probability) of the molecular structure of the (*S*,*S*)-2,4-dicyclohexyl-1-(3-phenylpropyl)phosphetane−borane complex **6a** in the solid state. Hydrogen atoms have been omitted for clarity.

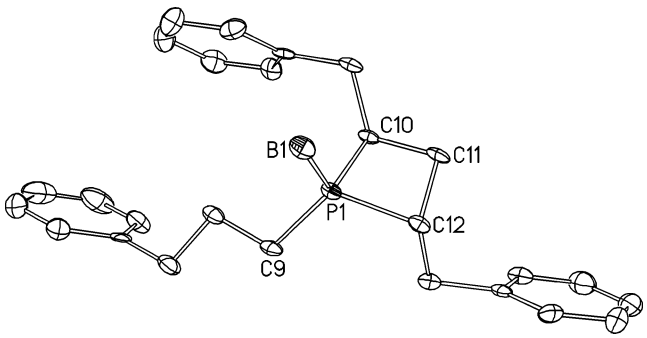

Figure 3. Thermal ellipsoid plot (50% probability) of the molecular structure of the (*S*,*S*)-2,4-dibenzyl-1-(3-phenylpropyl)phosphetane−borane complex **6d** in the solid state. Hydrogen atoms have been omitted for clarity.

Table 2. Crystallographic Data for 5c and 6a,d

	5c	6a	6d
empirical formula	$C_{11}H_{22}O_4S$	$C_{24}H_{40}BP$	$C_{26}H_{32}BP$
formula wt	250.35	370.34	386.30
color, form	colorless, plate	colorless, irreg	colorless, plate
size, mm	0.45 × 0.25 × 0.05	0.39 × 0.23 × 0.08	0.44 × 0.16 × 0.04
cryst syst	orthorhombic	orthorhombic	orthorhombic
space group	$P2_12_12_1$	$P2_12_12_1$	$P2_12_12_1$
a, Å	6.1801(3)	9.710(1)	6.414(1)
b, Å	11.2810(8)	12.271(1)	12.288(3)
c, Å	19.654(2)	19.457(2)	29.440(6)
α, deg	90	90	90
β, deg	90	90	90
γ, deg	90	90	90
V, Å^3	1370.2(2)	2318.3(4)	2320.3(8)
Z	4	4	4
ρ_{calcd}, g cm^{-3}	1.214	1.061	1.106
μ, mm^{-1}	0.234	0.124	0.127
abs cor T_{min}/T_{max}	0.745/1.000	none	0.930/1.000
no. of refined params	151	236	254
F(000)	544	816	832
no. of rflns measd	11 438	19 422	16 863
no. of indep rflns	2738	5004	3897
no. of obsd rflns ($I > 2\sigma(I)$)	2149	3686	2968
goodness of fit at F^2	1.092	0.990	1.085
R1 ($I > 2\sigma(I)$)	0.0496	0.0540	0.0582
wR2 (all data)	0.1054	0.1093	0.1167
abs structure param[36]	0.06(12)	0.06(11)	0.09(14)
max, min resid density, e Å^{-3}	0.539, −0.502	0.249, −0.316	0.385, −0.347

respectively, for **6a**,**d**), larger P−C−C angles (86.85−89.55°), and the largest values for the C−C−C angles (98.50 and 97.82°).

Quantitative generation of the free phosphetanes from borane complexes **6a**−**c** was achieved by reaction with Dabco at 40 °C in toluene.[30] Phosphetanes **7a**−**c** were obtained as colorless oils after filtration on a small alumina column and used without further purification. The reactions were monitored by $^{31}P\{^1H\}$ NMR spectroscopy. As expected, the quadrupole-broadened peaks of the borane adducts were replaced by sharp singlets at higher field between 17.3 and 21.6 ppm.

$[\{RuCl_2(\eta^6\text{-}C_6H_5COOMe)\}_2]$ (**8**) was chosen as the organometallic precursor for our investigations.[1] The (*S*,*S*)-(3-phenylpropyl)phosphetanes **7a**−**c** (**L***) were reacted with the ruthenium complex by adding their CH_2Cl_2 solutions to suspensions of **8** in the same solvent and stirring the reaction mixture at room temperature. As indicated by $^{31}P\{^1H\}$ NMR spectroscopy, the

(29) Gao, Y.; Sharpless, K. B. *J. Am. Chem. Soc*. **1988**, *110*, 7538.
(30) (a) Imamoto, T.; Kusumoto, N.; Suzuki, N.; Sato, K. *J. Am. Chem. Soc*., **1985**, *107*, 5301. (b) Brisset, H.; Gourdel, Y.; Pellon, P.; Le Corre, M. *Tetrahedron Lett*. **1993**, *34*, 4523.

Scheme 3

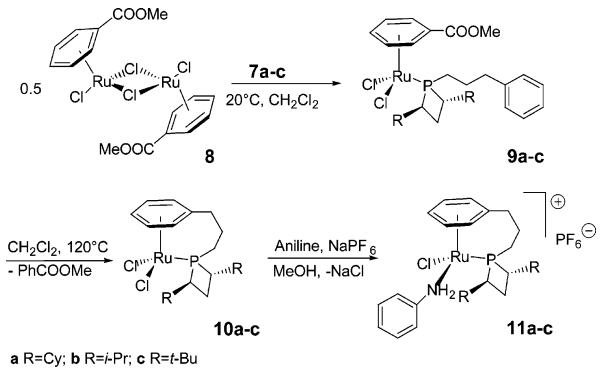

phosphetanes split complex dimer **8** and form the respective mononuclear σ-complex series [$RuCl_2$(η^6-C_6H_5COOMe)(η^1-**L***)] (**9a**−**c**) (Scheme 3). The η^6-arene methyl benzoate ligand is known to be labile at Ru(II) centers at elevated temperatures;[1,17,18] thus, **9a**−**c** are prone to an intramolecular arene exchange reaction, which led to the desired formation of the P-tethered complex family [$RuCl_2$(η^6:η^1-**L***)] (**10a**−**c**) within 1 day at 120 °C in dichloromethane in a sealed tube. The brown raw products were purified by chromatography to give **10a**−**c** as orange solids in 38−43% yield. **10a**−**c** are highly soluble in dichloromethane, soluble in diethyl ether, and sparingly soluble in *n*-hexane. Orange microcrystals were isolated from THF/pentane.

^{1}H, ^{13}C, and ^{31}P NMR spectra of complexes **10a**−**c** provided clear evidence for the η^6:η^1 coordination of the two designed ligand functions of **L*** = **7a**−**c**. The ^{1}H NMR spectra recorded for these complexes exhibit four resonances in the π-arene range between 4.78 and 6.29 ppm, which can be clearly attributed to an asymmetric η^6-phenyl group. The signals form one multiplet, two triplets, and one doublet of relative intensities 2:1:1:1, respectively. The ^{31}P NMR spectra of complexes **10a**−**c** displace only one singlet each between 63 and 72 ppm. The phosphorus chemical shifts are close to, though distinguishable from, those of the precursor σ-complexes **9a**−**c** (62−67 ppm), due to the σ-coordination of the phosphorus atoms in both classes of compounds.

Treatment of **10a**−**c** with 1 equiv of aniline at room temperature in the presence of $NaPF_6$ led to the substitution of a chloride ligand by the amine and the formation of the diastereomeric complex salts [RuCl(aniline)(η^6:η^1-**L***)]PF_6 (**11a**−**c**). Compounds **11a**−**c** are air-stable and can be crystallized from dichloromethane/hexane solutions as orange crystals in good yields (86−88%). An attempt to introduce a piperidine ligand in an analogous way did not result in the formation of a pure complex salt; instead, multicomponent mixtures were found.

The substitution of one of the two diastereotopic chloride ligands by aniline led to the desired stereogenic metal center, which combines with the two defined stereogenic centers of the phosphetanes **7a**−**c** to yield diastereomers. Due to the single-line absorption of each of the diastereomers, ^{31}P{^{1}H} NMR is the method of choice to determine the diastereoselectivity of the substitution reaction directly from the reaction mixtures. As was hoped for, good diastereoselectivities (84−88% de) were obtained.

Single crystals suitable for X-ray structure analysis of the major diastereomers of the tethered arene ruthenium(II) complex salts **11a**−**c** have been obtained from dichloromethane/*n*-hexane solutions. In accordance with the high diastereoselectivity of the substitution reaction, the X-ray structure analyses reveal the presence of only one enantiomer in each of the determined

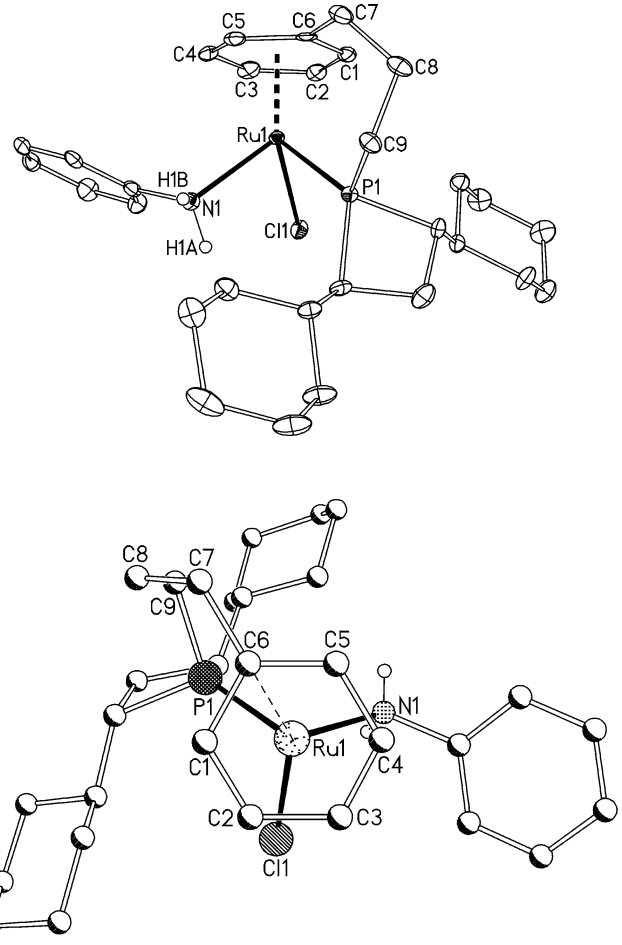

Figure 4. (top) Thermal ellipsoid plot (50% probability) of a side view of the complex cation of (R_{Ru},S_C,S_C)-[RuCl(aniline)(η^6:η^1-**L***)][PF_6] (**11a**; R = Cy) in the solid state. (bottom) Ball and stick model of its top view. C-bound hydrogen atoms have been omitted for clarity; the dashed line of the top view indicates the projection of the bond Ru(1)−C(6) on the ring plane.

crystal structures. All three salts crystallize in chiral space groups, **11a**,**b** in $P2_1$ and **11c** in $C2$, and a refinement of the Flack parameter[31] proves the correct determination of the absolute structure. The unit cells of **11b**,**c** contain two independent sets of ions in their asymmetric unit, representing the same enantiomer of the cations and differing only marginally in their conformations. The molecular structures of the complex cations of **11a**−**c** are presented in Figures 4−6, respectively. Selected bond distances and angles are reported in Table 3, and the crystallographic data are given in Table 4. The complexes have the expected piano-stool geometry, with the η^6-C_6H_5 rings occupying the facial coordination site. The η^6-coordinated phenyl groups are almost planar, with a clear trend in the Ru−C(arene) bond distances. The Ru−C bonds opposite to the P-donor atom (C(3) and C(4) in all three cases) are all longer (2.25−2.28 Å) than the other four bonds (2.18−2.22 Å). This documents a significant trans influence of the phosphetane ligand function, which has already been noticed in other tethered and nontethered [$Ru^{II}L_2$(arene)(PR_3)] complexes.[1,14,16,18,19] In addition, the benzylic carbon atoms C(7) of the side chains are situated within the ring plane of the arene ligands, thus documenting the absence of significant ring strain within the tether.

(31) Flack, H. D. *Acta Crystallogr.* **1983**, *A39*, 876.

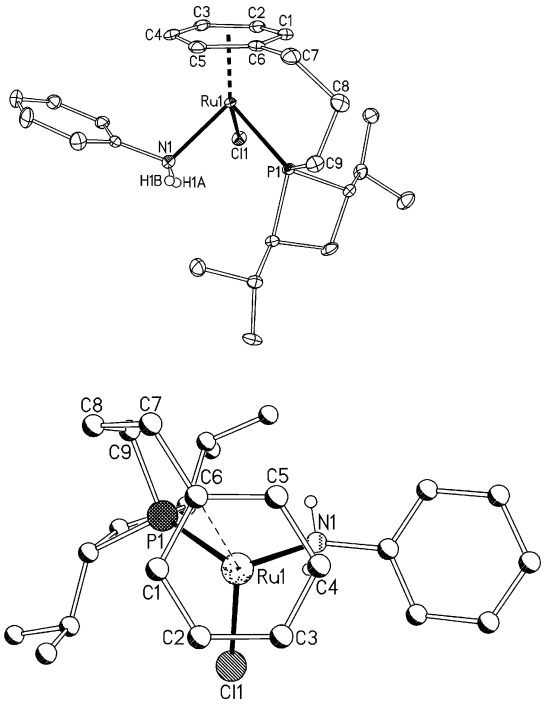

Figure 5. (top) Thermal ellipsoid plot (50% probability) of a side view of the complex cation of (R_{Ru},S_C,S_C)-[RuCl(aniline)(η^6:η^1-**L***)][PF_6] (**11b**; R = *i*-Pr) in the solid state. (bottom) Ball and stick model of its top view. C-bound hydrogen atoms have been omitted for clarity; the dashed line of the top view indicates the projection of the bond Ru(1)−C(6) on the ring plane.

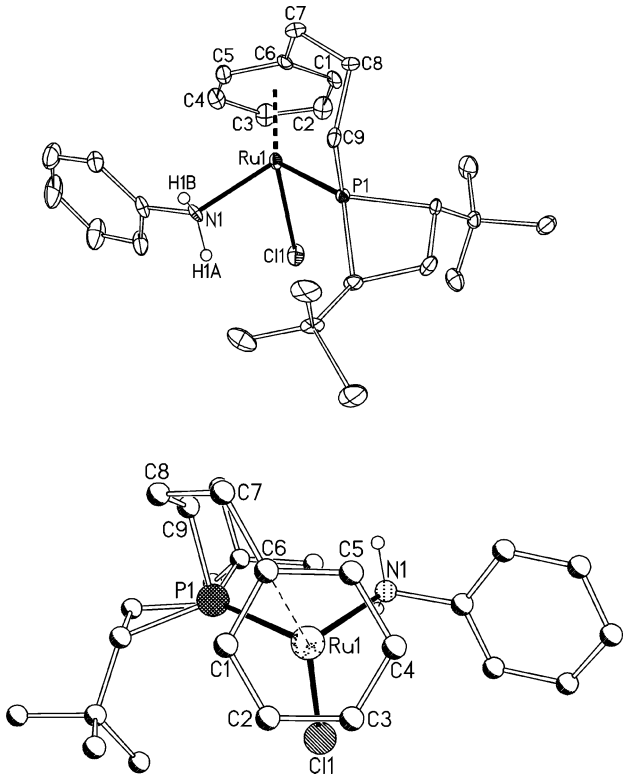

Figure 6. (top) Thermal ellipsoid plot (50% probability) of a side view of the complex cation of (R_{Ru},S_C,S_C)-[RuCl(aniline)-(η^6:η^1-**L***)][PF_6] (**11c**; R = *t*-Bu) in the solid state. (bottom) Ball and stick model of its top view. C-bound hydrogen atoms have been omitted for clarity; the dashed line of the top view indicates the projection of the bond Ru(1)−C(6) on the ring plane.

On the other hand, the tethered side chains of **11a**−**c** twist the piano-stool building block with respect to the arene ligand function, always in the same direction but in different magnitudes. The twist effect can be quantified by determining the angles between the projections of the bonds Ru(1)−P(1) and Ru(1)−C(6) on the planes of the phenyl groups, which should result in a single line in the absence of a twist. A graphical representation for the effect is given by the top views of the cations (Figures 4−6). The phosphetane phosphorus atom P(1) is positioned always at the left-hand side of the ring carbon atom C(6), forming twist angles between 23° (**11b**) and 39° (**11c**) (Table 5).

When we define a plane by the coordinates of the ruthenium and phosphorus atoms together with the center of the phenyl ring, a significant tilt of the phosphetane moiety can be found for the complex cations. As a consequence of this tilt and the *S*,*S* stereochemistry of the heterocycle, the phosphetane substituents occupy distinct spatial positions: one substituent is located mainly in a horizontal plane, which is defined by the three σ-donor atoms, but the other substituent points clearly to the space below.

The sum of the σ-ligand−Ru(1)−σ-ligand bond angles of **11a**−**c** should be influenced by the bulkiness of the phosphetane substituents, and the same should apply to the Ru(1)−P(1) bond distance. The sum parameter and Ru(1)−P(1) both have their maximum values for the *t*-Bu derivative **11c** (Table 5). Interestingly, the bulkiness of the phosphetane substituents controls the twist angle of the piano stool as well. The largest value of 39° again corresponds to **11c**.

According to the Cahn−Ingold−Prelog rules, the investigated major diastereomers of salts **11a**−**c** have all three the same *R* configuration at the ruthenium metal center. The complete stereochemical notation for these diastereomers is therefore R_{Ru},S_C,S_C.

Table 3. Selected Bond Distances (Å) and Angles (deg) for 11a−c

11a		**11b**		**11c**·0.5CH_2Cl_2	
		Bond Distances			
Ru(1)−C(1)	2.209(2)	Ru(1)−C(1)	2.217(3)	Ru(1)−C(1)	2.202(5)
Ru(1)−C(2)	2.184(2)	Ru(1)−C(2)	2.198(3)	Ru(1)−C(2)	2.197(6)
Ru(1)−C(3)	2.269(3)	Ru(1)−C(3)	2.265(3)	Ru(1)−C(3)	2.269(5)
Ru(1)−C(4)	2.272(2)	Ru(1)−C(4)	2.260(3)	Ru(1)−C(4)	2.281(5)
Ru(1)−C(5)	2.212(2)	Ru(1)−C(5)	2.190(3)	Ru(1)−C(5)	2.182(5)
Ru(1)−C(6)	2.228(2)	Ru(1)−C(6)	2.219(3)	Ru(1)−C(6)	2.202(5)
Ru(1)−Cl(1)	2.4094(5)	Ru(1)−Cl(1)	2.4110(7)	Ru(1)−Cl(1)	2.398(2)
Ru(1)−N(1)	2.175(2)	Ru(1)−N(1)	2.160(2)	Ru(1)−N(1)	2.184(4)
Ru(1)−P(1)	2.3269(7)	Ru(1)−P(1)	2.3168(7)	Ru(1)−P(1)	2.351(2)
		Bond Angles			
P(1)−Ru(1)−Cl(1)	83.78(3)	P(1)−Ru(1)−Cl(1)	87.17(3)	P(1)−Ru(1)−Cl(1)	87.59(4)
N(1)−Ru(1)−Cl(1)	80.91(5)	N(1)−Ru(1)−Cl(1)	80.77(7)	N(1)−Ru(1)−P(1)	82.8(2)
N(1)−Ru(1)−P(1)	92.04(5)	N(1)−Ru(1)−P(1)	87.04(6)	N(1)−Ru(1)−P(1)	90.7(2)
C(7)−C(8)−C(9)	113.5(2)	C(7)−C(8)−C(9)	112.2(2)	C(7)−C(8)−C(9)	114.6(4)

Table 4. Crystallographic Data for 11a−c

	11a	11b	11c
empirical formula	$C_{30}H_{44}ClF_6NP_2Ru$	$C_{24}H_{36}ClF_6NP_2Ru$	$C_{26.5}H_{41}Cl_2F_6NP_2Ru$
formula wt	731.12	651.00	721.51
color, form	orange, prisms	orange, blocks	orange, blocks
size, mm	0.26 × 0.23 × 0.15	0.25 × 0.23 × 0.21	0.37 × 0.18 × 0.10
cryst syst	monoclinic	monoclinic	monoclinic
space group	$P2_1$	$P2_1$	$C2$
a, Å	9.3472(7)	10.3198(8)	19.012(2)
b, Å	13.2935(7)	20.126(2)	10.631(1)
c, Å	12.8177(7)	13.0266(4)	31.003(3)
α, deg	90	90	90
β, deg	98.811(5)	93.332(4)	97.201(8)
γ, deg	90	90	90
V, Å^3	1573.9(2)	2701.0(4)	6216.8(9)
Z	2	4	8
ρ_{calcd}, g cm^{-3}	1.543	1.601	1.542
μ, mm^{-1}	0.742	0.854	0.833
abs cor T_{min}/T_{max}	0.858/1.000	0.869/1.000	0.811/0.929
no. of refined params	370	639	734
F(000)	752	1328	2952
no. of rflns measd	33 080	62 216	41 871
no. of indep rflns	9570	15 593	11 249
no. of obsd rflns ($I > 2\sigma(I)$)	7961	13037	8733
goodness of fit at F^2	0.895	0.859	0.937
R1 ($I > 2\sigma(I)$)	0.0334	0.0353	0.0422
wR2 (all data)	0.0669	0.0711	0.0856
abs structure param[36]	−0.006(17)	−0.018(14)	−0.03(2)
max, min resid density, e Å^{-3}	0.499, −0.645	0.501, −0.509	0.725, −0.744

Table 5. Selected Structural Data of Complex Salts 11a−c

	11a	11b	11c
∑ σ-L−Ru−σ-L bond angles (deg)	256.65	254.90	261.06
Ru−P(1) (Å)	2.326	2.317	2.351
twist angle (deg)	25	23	39

The NMR spectroscopic properties of all arene ruthenium(II) complexes presented in this paper indicate an undisturbed diamagnetism and, thus, low-spin d^6 configurations. σ-Ligand exchange reactions of such closed-shell piano-stool species normally follow a dissociative mechanism. Therefore, the stereoselectivity of the chloride substitution process of [RuCl$_2$(η^6:η^1-**L***)] (**10**) should be related to the stereochemical properties of the proposed intermediate, the dechlorinated 16-valence-electron complex cation [RuCl(η^6:η^1-**L***)]$^+$ ([**12**]$^+$).[32]

To evaluate this assumption, density functional theory (DFT) calculations have been performed in order to investigate the structures of the *t*-Bu complex [RuCl$_2$(η^6:η^1-**L***)] (**10c**) and its postulated monochloride intermediate of the chloride substitution reaction, [RuCl(η^6:η^1-**L***)]$^+$ ([**12c**]$^+$), to get to salt **11c** in a diastereoselective way. This system has been chosen since it shows the largest deviation from the symmetrical bond situation. All calculations have been done with the DFT modules of the program package Turbomole[33] employing the BP86 density functional[34] and a basis set of polarized valence triple-ζ quality (TZVP)[35] within the RI (resolution of identity) approximation.[36] An effective core potential which accounts for the most important relativistic effects has been used for ruthenium.[37] A clear steric discrimination of the diastereotopic sides of neutral complex **10c** is observed (Figure 7). Selected bond distances and angles for the calculated structures are summarized in Table 6.

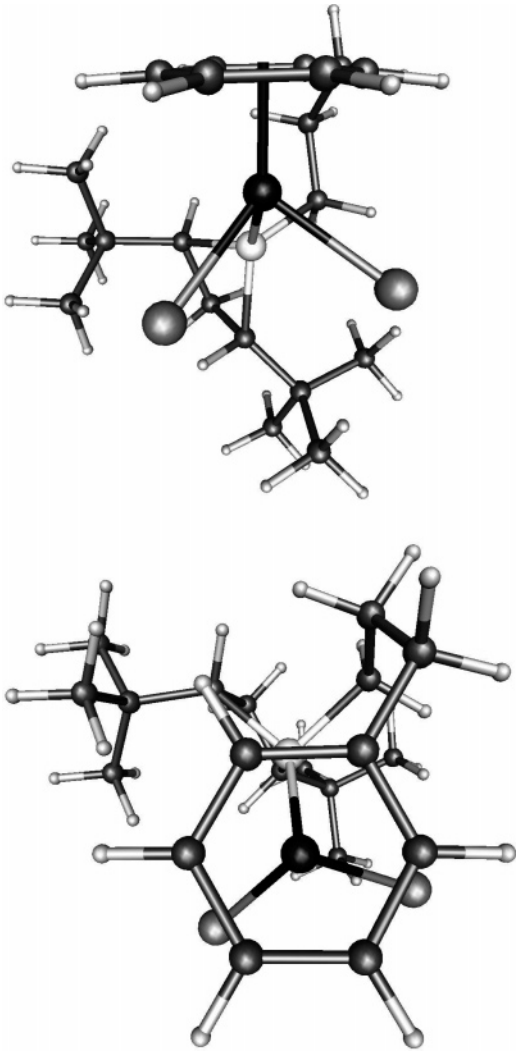

Figure 7. Calculated molecular structure of [RuCl$_2$(η^6:η^1-**L***)] (**10c**; R = *t*-Bu): (top) side view; (bottom) top view.

The framework of the (η^6:η^1-arene∩donor)Ru moiety remains quite stable for the monochloride cation [**12**]$^+$, as compared to the calculated values of **10c** and the experimental data for the cation of **11c**. The molecular structure of [**12**]$^+$ (Figure 8) suggests an easier attack of an incoming ligand on the metal atom from the pro-R_{Ru} side, which leads to the R_{Ru},S_C,S_C diastereomer. The phosphetane *t*-Bu substituent at this side of the intermediate complex is oriented nicely out of the way of an incoming nucleophile; however, that is a kinetic consideration.

A related approach was utilized to investigate the relative thermodynamic stabilities of the R_{Ru},S_C,S_C and S_{Ru},S_C,S_C diastereomers of salt **11c** theoretically. To exclude basis set dependent effects, a smaller basis set of split valence quality with polarization functions on all heavy atoms, denoted as SV(P),[38] was also utilized. The B3LYP hybrid density functional[39]

(32) Dadci, L.; Elias, H.; Frey, U.; Hornig, A.; Koelle, U.; Merbach, A. E.; Paulus, H.; Schneider, J. S. *Inorg. Chem.* **1995**, *34*, 406.
(33) (a) Ahlrichs, R.; Bär, M.; Häser, M.; Horn, H.; Kölmel, C. *Chem. Phys. Lett.* **1989**, *162*, 165. (b) http://www.turbomole.com.
(34) (a) Vosko, S.; Wilk, L.; Nusair, M. *Can. J. Phys.* **1980**, *58*, 1200. (b) Becke, A. D. *Phys. Rev. A* **1988**, *38*, 3098. (c) Perdew, J. P. *Phys. Rev. B* **1986**, *33*, 8822.
(35) Schäfer, A.; Huber, C.; Ahlrichs, R. *J. Chem. Phys.* **1994**, *100*, 5829.
(36) Eichkorn, K.; Weigend, F.; Treutler, O. A.; Ahlrichs, R. *Theor. Chem. Acc.* **1997**, *97*, 119.
(37) Andrae, D.; Häusser, M.; Dolg, M.; Stoll, H. *Theor. Chim. Acta* **1990**, *77*, 126.
(38) Schäfer, A.; Horn, H.; Ahlrichs, R. *J. Chem. Phys.* **1992**, *97*, 2571.

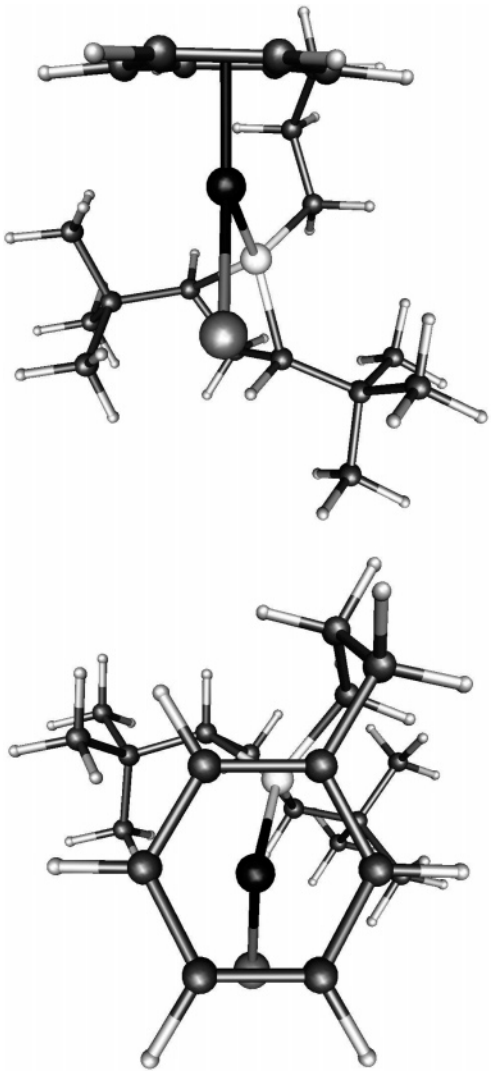

Figure 8. Calculated molecular structure of [RuCl(η^6:η^1-**L***)]$^+$ (**12**; R = *t*-Bu): (top) side view; (bottom) top view.

Table 6. Calculated Bond Distances (Å) and Bond Angles (deg) for Complex 10c and Its Dechlorination Product [12]$^+$

10c		[**12**]$^+$	
Bond Distances			
Ru(1)−C(1)	2.194	Ru(1)−C(1)	2.236
Ru(1)−C(2)	2.225	Ru(1)−C(2)	2.184
Ru(1)−C(3)	2.283	Ru(1)−C(3)	2.291
Ru(1)−C(4)	2.291	Ru(1)−C(4)	2.254
Ru(1)−C(5)	2.191	Ru(1)−C(5)	2.153
Ru(1)−C(6)	2.218	Ru(1)−C(6)	2.249
Ru(1)−Cl(1)	2.435	Ru(1)−Cl(1)	2.492
Ru(1)−N(1)	2.435	Ru(1)−N(1)	
Ru(1)−P(1)	2.336	Ru(1)−P(1)	2.375
Bond Angles			
P(1)−Ru(1)−Cl(1)	82.483	P(1)−Ru(1)−Cl(1)	87.15(3)
N(1)−Ru(1)−Cl(1)	89.424		
N(1)−Ru(1)−P(1)	87.047		

as implemented in Turbomole was additionally employed to reduce the bias due to the density functional. A harmonic frequency analysis has been performed for both diastereomers R_{Ru} and S_{Ru} at the BP86/RI/TZVP level of theory. The force constants were obtained as numerical first derivatives of the analytical energy gradients, as implemented in the parallel PVM code SNF.[40] In addition to characterizing the stationary points on the potential energy surface as true minima, the harmonic frequency analysis yields the zero-point energy (ZPE) and thermal corrections. Selected structural parameters of the two diastereomeric cations R_{Ru} and S_{Ru} as calculated at the BP86/RI/TZVP level of theory are presented in Table 7.

Table 7. Calculated Bond Distances (Å) and Bond Angles (deg) for Two Diastereomers of Complex Cation [11c]$^+$

[**11c**]$^+$ (R_{Ru})		[**11c**]$^+$ (S_{Ru})	
Bond Distances			
Ru(1)−C(1)	2.236	Ru(1)−C(1)	2.215
Ru(1)−C(2)	2.218	Ru(1)−C(2)	2.248
Ru(1)−C(3)	2.296	Ru(1)−C(3)	2.298
Ru(1)−C(4)	2.299	Ru(1)−C(4)	2.296
Ru(1)−C(5)	2.231	Ru(1)−C(5)	2.208
Ru(1)−C(6)	2.254	Ru(1)−C(6)	2.244
Ru(1)−Cl(1)	2.421	Ru(1)−Cl(1)	2.417
Ru(1)−N(1)	2.190	Ru(1)−N(1)	2.194
Ru(1)−P(1)	2.378	Ru(1)−P(1)	2.372
Bond Angles			
P(1)−Ru(1)−Cl(1)	88.79	P(1)−Ru(1)−Cl(1)	84.40
N(1)−Ru(1)−Cl(1)	78.74	N(1)−Ru(1)−Cl(1)	80.78
N(1)−Ru(1)−P(1)	90.85	N(1)−Ru(1)−P(1)	90.14

Table 8. Relative Energies of the Diastereomers of Complex Cation [11c]$^+$ (R_{Ru})

basis set	method	ΔE (kJ mol^{-1})
SV(P)	BP86/RI	−0.3
	B3LYP	−0.5
TZVP	BP86/RI	0.7
	B3LYP	1.0

A good agreement between the calculated and the experimental structural parameters of the R_{Ru} diastereomer is an indication for the reliability of the calculations. All bond distances and bond angles match within 0.006−0.052 Å and 0.16−4.04°, respectively. This includes the trans influence of the phosphorus atom. As for the R_{Ru},S_C,S_C diastereomer of complex **11c** experimentally verified, the calculated bond distances Ru−C(3) and Ru−C(4) are the longest Ru−C(arene) distances of the complex.

The relative energies of the R_{Ru} and S_{Ru} diastereomers of the complex cation [RuCl(aniline) (η^6:η^1-**L***)]$^+$ ([**11c**]$^+$), as calculated by the different levels of theory, are presented in Table 8, and the total energies of the R_{Ru} species have been taken as references. The ZPE and Gibbs enthalpy at 298 K have been calculated at the BP86/RI/TZVP level of theory. Their relative values amount to −0.6 and −0.5 kJ mol^{-1}, respectively.

While the SV(P) basis set predicts the S_{Ru} diastereomer to be slightly more stable, the TZVP basis set favors the R_{Ru} diastereomer. This almost isoenergetic situation for the two diastereomers excludes a thermodynamic control of the ligand exchange reaction and points toward a kinetic effect.

Conclusions

The enantiopure 2,4-disubstituted 1-(3-phenylpropyl)phosphetane derivatives **7a**−**c** (R = Cy, *i*-Pr, *t*-Bu) have been successfully designed and prepared to form configurationally stable (*S*,*S*)-(η^6:η^1-arene∩phosphetane*)Ru complexes. The rational approach to **7a**−**c** is based on the reaction between (3-phenylpropyl)phosphane with the chiral cyclic (*R*,*R*)-sulfates **5a**−**c**, which takes place with inversion of the stereogenic centers. The complexes (S_C,S_C)-[RuCl$_2${2,4-R$_2$-1-(η^6-3-phenylpropyl)-η^1-phosphetane}] (**10a**−**c**) allow a diastereoselective

(39) Becke, A. D. *J. Chem. Phys.* **1993**, *98*, 5648.

(40) Neugebauer, J.; Reiher, M.; Kind, C.; Hess, B. A. *J. Comput. Chem.* **2002**, *23*, 895.

nucleophilic substitution of one of the two diastereotopic chloride ligands by aniline. The main products are the salts (R_{Ru},S_C,S_C)-[RuCl(aniline){2,4-R_2-1-(η^6-3-phenylpropyl)-η^1-phosphetane}]PF_6 (**11a**−**c**).

A theoretical approach for the explanation of the diastereoselectivity utilized DFT calculations on the dechlorinated 16-valence-electron intermediate cation of the substitution reaction, (S_C,S_C)-[RuCl{2,4-di-*tert*-butyl-1-(η^6-3-phenylpropyl)-η^1-phosphetane}]$^+$ ([**12**]$^+$). As for the experimental findings, the theoretical results are strongly in favor of an attack of an incoming ligand on the pro-R_{Ru} side. Investigation of the relative stabilities of the R_{Ru} and S_{Ru} diastereomers of the complex cation [**11c**]$^+$ revealed an isoenergetic situation. Thus, the ligand exchange reaction is unlikely to be thermodynamically controlled. Experiments on the catalytic properties of salts **11a**−**c** as hydrogen transfer catalysts are in progress.

Experimental Section

All reactions involving organometallic compounds were carried out under a dry nitrogen or argon atmosphere, using conventional Schlenk-tube techniques. The tethered arene ruthenium(II) complexes are robust compounds, air stable in the solid state and only slightly air sensitive in solution. Solvents were dried and degassed before use. NMR spectra were recorded at room temperature on JEOL FT-JNM-EX 270, JEOL FT-JNM-LA 400, and Bruker Advance DPX 300 spectrometers, using dimethylpolysiloxane and solvent signals as internal standards. Mass spectra were recorded on a Varian MAT 212 spectrometer, microanalyses were performed using a Carlo Erba Model 1106 elemental analyzer, and polarimetric measurements were performed on a Perkin-Elmer polarimeter. The cyclic sulfates **5a**−**e** [23,24,27] and 3-(methoxycarbonyl)cyclohexa-1,4-diene[41] (**8**) were prepared as reported in the literature.

(3-Phenylpropyl)phosphane (4). A solution of (3-phenylpropyl)-magnesium bromide (60 mL) in diethyl ether, prepared by the reaction of magnesium turnings (1.45 g, 0.05 mol) with (3-phenypropyl)bromide (10 g, 7.63 mL, 0.05 mol) in refluxing anhydrous diethyl ether (80 mL), was added slowly at 0 °C to a solution of PCl_3 (7.60 g, 5 mL, 0.055 mol) in diethyl ether (10 mL). The reaction mixture was warmed slowly to room temperature and stirred overnight. After filtration the solvent was removed under vacuum to give a yellow residual oil, which was used without purification. A solution of the yellow oil in diethyl ether (15 mL) was added dropwise to a stirred suspension of an excess of $LiAlH_4$ in diethyl ether (120 mL) at 0 °C. After the addition was complete, stirring was continued at 0 °C for 1 h. The reaction mixture was warmed to room temperature and then refluxed for 2 h. After the mixture was cooled to 0 °C, a 37% aqueous solution of HCl (20 mL) was carefully added. The organic layer was extracted with ether and dried with magnesium sulfate. **4** was obtained as a colorless oil after distillation at 65−70 °C/ 1.5×10^{-2} mbar (3.65 g, 48% yield).

Data for **4**: ^{1}H NMR (300.1 MHz, $CDCl_3$, δ) 7.31−7.20 (m, 5H, Ph), 2.75 (d, $^1J_{PH}$ = 194.5 Hz, 2H, PH), 2.72 (t, 2H, CH_γ), 1.95−1.82 (m, 2H, CH_β), 1.56 (br, 2H, CH_α); ^{13}C{^{1}H} NMR (67.7 MHz, $CDCl_3$, δ): 141.66 (Ph, C_{ipso}), 128.40 (Ph), 128.25 (Ph), 125.76 (Ph), 36.76 (d, $^2J_{PC}$ = 5.5 Hz, C_β), 34.71 (d, $^3J_{PC}$ = 3.0 Hz, C_γ), 13.41 (d, $^1J_{PC}$ = 7.4, C_α); ^{31}P{^{1}H} NMR (121.5 MHz, $CDCl_3$, δ) −136.20.

(*S*,*S*)-2,4-R_2-1-(3-phenylpropyl)phosphetane−Borane Complexes 6a−c. General Procedure. To a mixture of (3-phenylpropyl)phosphane (1 mmol) and the respective cyclic (*R*,*R*)-sulfates **5a**−**d** (1.1 equiv) in THF (35 mL) at −78 °C was carefully added 2.2 equiv of 1.6 M *n*-BuLi, and the mixture was stirred for 30 min without temperature change. The solution was warmed slowly to room temperature, and after it was stirred for about 2 h, 2 equiv of BH_3·SMe_2 was added. After addition of water (ca. 2 mL) the solvents were removed under vacuum, the residue was extracted with ethyl ether, and the extract was washed with water and dried with $MgSO_4$. Subsequently the solvent was removed at reduced pressure to isolate the products.

(*S*,*S*)-2,4-Dicyclohexyl-1-(3-phenylpropyl)phosphetane−Borane Complex 6a. The (*R*,*R*)-1,3-dicyclohexylpropane-1,3-diol cyclic sulfate **5a** was used in this experiment. Recrystallization from ether−hexane gave **6a** as a colorless crystalline solid (0.24 g, 66% yield).

Data for **6a**: ^{1}H NMR (300.1 MHz, CD_2Cl_2, δ) 7.24−7.09 (m, 5H, Ph), 2.68−2.58 (m, 2H), 2.35−2.09 (m, 3H), 1.99−1.02 (m, 25H), 0.86−0.60 (m, 5H); ^{13}C{^{1}H} NMR (75.5 MHz, CD_2Cl_2, δ) 141.66 (Ph, C_{ipso}), 128.72 (Ph), 128.68 (Ph), 126.31 (Ph), 39.36 (d, J = 35.6 Hz, CH), 39.05 (CH), 38.29 (CH), 38.11 (d, J = 37.8 Hz, CH), 37.49 (d, J_{CP} = 12.3 Hz, CH_2), 32.89 (d, J_{CP} = 3.6 Hz, CH_2), 32.53 (d, J_{CP} = 4.4 Hz, CH_2), 31.15 (d, J_{CP} = 12.3 Hz, CH_2), 30.72 (d, J_{CP} = 11.6 Hz, CH_2), 28.93 (d, J_{CP} = 16.7 Hz, CH_2), 26.64, 26.49, 26.31, 26.19, 26.04, 25.91 (CH_2), 25.14 (CH_2), 22.02 (d, J_{CP} = 19.6 Hz, CH_2); ^{31}P{^{1}H} NMR (121.5 MHz, CD_2Cl_2, δ) 53.4 (J_{PB}= 52 Hz); MS (FD, 2kV, *m*/*z*) 370 [M$^+$]; $[\alpha]_D$ = +40.63° (c = 0.88, CH_2Cl_2).

(*S*,*S*)-2,4-Diisopropyl-1-(3-phenylpropyl)phosphetane−Borane Complex 6b. The (*R*,*R*)-2,6-dimethylheptane-3,5-diol cyclic sulfate **5b** was used in this case. **6b** forms a colorless oil (0.13 g, 42% yield).

Data for **6b**: ^{1}H NMR (300.1 MHz, $CDCl_3$, δ) 7.12−6.92 (m, 5H, Ph), 2.55−2.47 (m, 2H), 2.20−1.47 (m, 10H), 1.07−0.83 (m, 12H, CH_3); ^{13}C{^{1}H} NMR (75.5 MHz, $CDCl_3$, δ) 140.55 (C_{ipso}, Ph), 128.07 (superposed, Ph), 128.02 (Ph), 125.74 (Ph), 39.98 (d, J_{CP} = 39.9 Hz, CH), 38.75 (d, J_{CP} = 37.1 Hz, CH), 36.83 (d, J_{CP} = 12.4 Hz, CH_2), 30.55 (d, J_{CP} = 15.9 Hz, CH_2), 29.94 (d, J_{CP} = 5.1 Hz, CH), 29.36 (CH), 24.9 (CH_2), 22.41 (d, superposed, J_{CP} = 3.6 Hz, CH_3), 22.07 (d, J_{CP} = 20.4 Hz, CH_2), 20.89 (d, J_{CP} = 12.4 Hz, CH_3), 20.57 (d, J_{CP} = 11.6 Hz, CH_3); ^{31}P{^{1}H} NMR (121.5 MHz, CD_2Cl_2, δ) 52.64 (d, J_{PB} = 52 Hz); MS (FD, 2kV, *m*/*z*) 290 [M$^+$]; $[\alpha]_D$ = +116.67° (c = 0.1, CH_2Cl_2).

(*S*,*S*)-2,4-Di-*tert*-butyl-1-(3-phenylpropyl)phosphetane−Borane Complex 6c. The (*R*,*R*)-2,2,6,6-tetramethylheptane-3,5-diol cyclic sulfate **5c** was used in this case. **6c** forms a colorless oil (0.06 g, 20% yield).

Data for **6c**: ^{1}H NMR (270.2 MHz, $CDCl_3$, δ) 7.35−7.10 (m, 5H, Ph), 2.80−2.61 (m, 2H), 2.11−2.06 (m, 4H), 1.32−0.80 (m, 22H); ^{13}C{^{1}H} NMR (75.5 MHz, $CDCl_3$, δ) 141.02 (C_{ipso}, Ph), 128.32 (Ph), 128.15 (Ph), 125.92 (Ph), 32.80 ($C(CH_3)$), 31.86 ($C(CH_3)$), 28.94 (d, J_{CP} = 5.8 Hz, $C(CH_3)$), 28.30 (d, J_{CP} = 5.8 Hz, $C(CH_3)$), 27.29 (CH_2), 26.32 (superposed CH_2), 26.11 (CH_2); ^{31}P{^{1}H} NMR (161.7 MHz, $CDCl_3$, δ) 53.21 (br); MS (FD, 2kV, *m*/*z*) 318 [M$^+$]; $[\alpha]_D$ = +29.78° (c = 3.7, CH_2Cl_2).

(*S*,*S*)-2,4-Dibenzyl-1-(3-phenylpropyl)phosphetane−Borane Complex 6d. The (*R*,*R*)-1,5-diphenylpentane-2,4-diol cyclic sulfate **5d** was used in this case. The residue was purified by chromatography on an alumina column with hexane/diethyl ether (9:1). Recrystallization from ether/pentane afforded **6d** as a pure, white solid (0.07 g, 18% yield).

Data for **6d**: ^{1}H NMR (399.7 MHz, CD_2Cl_2, δ) 7.35−7.12 (m, 15H, Ph), 3.10−2.60 (m, 8H), 2.39−2.24 (m, 2H), 1.89−1.31 (m, 4H); ^{13}C{^{1}H} NMR (100.4 MHz, CD_2Cl_2, δ) 141.39 (Ph, C_{ipso}), 140.20 (d, J = 9.9 Hz, benzyl C_{ipso}), 139.28 (d, J = 9.1 Hz, benzyl C_{ipso}), 129.16−128.74 (superposed, Ph), 126.88−126.30 (superposed, Ph), 37.19 (d, J = 12.4 Hz, CH_2), 36.45 (CH_2), 35.69 (d, J = 5.0 Hz, CH_2), 34.53 (d, J_{CP} = 37.5 Hz, CH), 33.07 (d, J_{CP} = 38.8 Hz, CH), 31.46 (d, J_{CP} = 14.7 Hz, CH_2), 24.92 (CH_2), 22.78 (d, J_{CP} = 17.4 Hz, CH_2); ^{31}P{^{1}H} NMR (161.7 MHz, CD_2Cl_2, δ)

(41) Drew, M. G. B.; Reagan, C. M.; Nelson, S. M. *J. Chem. Soc., Dalton Trans.* **1980**, 1934.

50.65 (br); MS (FD, 2kV, *m*/*z*) 387 [M^+]; $[\alpha]_D = -5.18°$ ($c = 2.7$, CH_2Cl_2).

(*S*,*S*)-2,4-R_2-1-(3-phenylpropyl)phosphetanes 7a−c. General Procedure. The respective phosphetane−borane complexes (1 mmol) were treated with Dabco (1.1 equiv) in toluene (8 mL) at 50 °C for 3 h. The resulting reaction mixtures were transferred on top of a short alumina column for separation with hexane/diethyl ether (95:5) as eluent. After removal of the solvents at reduced pressure, the (phenylpropyl)phosphetanes were obtained as colorless oils in almost quantitative yields, as indicated by the single-line ^{31}P NMR spectra, and were used without further purification.

(*S*,*S*)-2,4-Dicyclohexyl-1-(3-phenylpropyl)phosphetane (7a): $^{31}P\{^1H\}$ NMR (109.4 MHz, CD_2Cl_2, δ) 17.26.

(*S*,*S*)-2,4-Diisopropyl-1-(3-phenylpropyl)phosphetane (7b): $^{31}P\{^1H\}$ NMR (121.5 MHz, CD_2Cl_2, δ) 17.35.

(*S*,*S*)-2,4-Di-*tert*-butyl-1-(3-phenylpropyl)phosphetane (7c): $^{31}P\{^1H\}$ NMR (109.4 MHz, $CDCl_3$, δ) 21.61.

[$RuCl_2$(η^6-C_6H_5COOMe){2,4-R_2-1-(3-phenylpropyl)-η^1-phosphetane}] (9a−c). General Procedure. A solution of the desired phosphetane (0.5 mmol) in CH_2Cl_2 (10 mL) was added to a suspension of the Ru complex dimer [$RuCl_2(C_6H_5COOMe)]_2$ (**8**; 0.5 equiv) in CH_2Cl_2 (20 mL). After it was stirred for 3 h at room temperature, the red solution was filtered and the solvent removed at reduced pressure. The residue was washed with hexane and diethyl ether several times and dried under vacuum. The complexes **9a**−**c** were obtained as red-orange oily solids in almost quantitative yields, as indicated again by the single-line ^{31}P NMR spectra, and were used without further purification.

[$RuCl_2$(η^6-C_6H_5COOMe){2,4-dicyclohexyl-1-(3-phenylpropyl)-η^1-phosphetane}] (9a): $^{31}P\{^1H\}$ NMR (121.5 MHz, CD_2Cl_2, δ) 67.00.

[$RuCl_2$(η^6-C_6H_5COOMe){2,4-diisopropyl-1-(3-phenylpropyl)-η^1-phosphetane}] (9b): $^{31}P\{^1H\}$ NMR (121.5 MHz, CD_2Cl_2, δ) 65.44.

[$RuCl_2$(η^6-C_6H_5COOMe){2,4-di-*tert*-butyl-1-(3-phenylpropyl)-η^1-phosphetane}] (9c): $^{31}P\{^1H\}$ NMR (121.5 MHz, $CDCl_3$, δ) 62.34.

(S_C,S_C)-[$RuCl_2$(2,4-R_2-1-{η^6-3-phenylpropyl}-η^1-phosphetane)] (10a−c). General Procedure. A solution of the desired arene−phosphetane complex **9** (1 mmol) in dichloromethane (20 mL) was heated in a Schlenk pressure glass tube at 120 °C for 24 h to form a brown solution. The solvent was removed under vacuum and the residue purified by chromatography on a silica column with acetone/ethyl acetonate (1:1) as eluent. Recrystallization from THF/pentane afforded pure complexes **10a**−**c** as orange solids.

[$RuCl_2${2,4-dicyclohexyl-1-(η^6-3-phenylpropyl)-η^1-phosphetane}] (10a):** yield 0.23 g, 43%; ^1H NMR (300.1 MHz, $CDCl_3$, δ) 6.20−6.12 (m, 2H, η^6-C_6H_5), 5.16 (t, 1H, η^6-C_6H_5), 4.89 (t, 1H, η^6-C_6H_5), 4.78 (d, 1H, η^6-C_6H_5), 2.72−2.67 (m, 2H, CH), 2.38−1.43 (m, 24H), 1.11−0.57 (m, 6H); $^{13}C\{^1H\}$ NMR (75.5 MHz, $CDCl_3$, δ) 100.36 (d, $J_{PC} = 10.2$ Hz, η^6-C_6H_5), 99.96 (d, $J_{PC} = 9.5$ Hz, η^6-C_6H_5), 89.46 (η^6-C_6H_5), 85.45 (η^6-C_6H_5), 81.50 (η^6-C_6H_5), 47.18 (d, $J_{PC} = 47.2$ Hz, CH), 38.87 (d, $J_{PC} = 28.3$ Hz, CH), 38.59 (CH), 38.21 (CH), 34.14 (d, $J_{PC} = 2.9$ Hz, CH_2), 33.52 (d, $J_{PC} = 4.4$ Hz, CH_2), 30.40, 30.26, 30.09, 29.97, 29.82 (CH_2), 29.16 (d, $J_{PC} = 13.8$ Hz, CH_2), 26.17, 26.05 (superposed, CH_2); 25.05, 25.81, 25.67 (CH_2), 23.53 (d, $J_{PC} = 8.7$ Hz, CH_2), 21.94 (CH_2); $^{31}P\{^1H\}$ NMR (121.5 MHz, $CDCl_3$, δ) 71.14; MS (FD, 2kV, *m*/*z*) 528 [M^+]. Anal. Found (calcd) for $C_{24}H_{37}Cl_2PRu$: C, 53.99 (54.54); H, 6.85 (7.06).

[$RuCl_2${2,4-diisopropyl-1-(η^6-3-phenylpropyl)-η^1-phosphetane}] (10b):** yield 0.21 g, 46%; ^1H NMR (300.1 MHz, $CDCl_3$, δ) 6.29−6.20 (m, 2H, η^6-C_6H_5), 5.29 (t, 1H, η^6-C_6H_5), 4.99 (t, 1H, η^6-C_6H_5), 4.88 (d, 1H, η^6-C_6H_5), 2.80−2.66 (m, 2H, CH), 2.48−1.91(m, 10 H, CH + CH_2), 0.95 (d, 3H, CH_3), 0.84 (d, 3H, CH_3), 0.82 (d, 3H, CH_3), 0.80 (d, 3H, CH_3); $^{13}C\{^1H\}$ NMR (75.5 MHz, $CDCl_3$, δ) 100.75 (d, $J_{CP} = 9.4$ Hz, Ph), 100.25 (d, $J_{CP} = 9.4$ Hz, Ph), 85.87 (Ph);, 81.74 (Ph), 78.12 (Ph), 77.20 (Ph);, 48.98 (d, $J_{CP} = 30.5$ Hz, CH), 39.73 (d, $J_{CP} = 34.9$ Hz, CH), 30.61 (d, $J_{CP} = 13.6$ Hz, CH_2), 30.28 (d, $J_{CP} = 1.5$ Hz, CH_2), 29.25 (d, $J_{CP} = 7.4$ Hz, CH), 29.01 (CH), 23.56 (d, $J_{CP} = 9.5$ Hz, CH_2), 23.34 (d, $J_{CP} = 3.6$ Hz, CH_3), 23.17 (d, $J_{CP} = 5.1$ Hz, CH_3), 22.07 (CH_2), 20.45 (d, partially superposed, $J_{CP} = 10.2$ Hz, CH_3), 20.16 (d, partially superposed, $J_{CP} = 12.4$ Hz, CH_3); $^{31}P\{^1H\}$ NMR (121.5 MHz, $CDCl_3$, δ) 68.85; MS (FD, 2kV, *m*/*z*) 448 [M^+]. Anal. Found (calcd) for $C_{18}H_{29}Cl_2PRu$: C, 48.59 (48.22); H, 6.70 (6.52).

[$RuCl_2${2,4-di-*tert*-butyl-1-(η^6-3-phenylpropyl)-η^1-phosphetane}] (10c):** yield 0.18 g, 38%; ^1H NMR (300.1 MHz, $CDCl_3$, δ) 6.29−6.19 (m, 2H, η^6-C_6H_5), 5.43 (t, 1H, η^6-C_6H_5), 5.00 (d, 1H, η^6-C_6H_5), 4.85 (t, 1H, η^6-C_6H_5), 2.80−2.68 (m, 2H, CH), 2.56−1.97 (m, 6H, CH_2), 0.98 (d, 18H, CH_3); $^{31}P\{^1H\}$ NMR (121.5 MHz, $CDCl_3$, δ) 63.47; MS (FD, 2kV, *m*/*z*) 476 [M^+]. Anal. Found (calcd) for $C_{20}H_{33}Cl_2PRu$: C, 49.99 (50.42); H, 7.10 (6.98).

(S_C,S_C)-[RuCl(aniline){2,4-R_2-1-(η^6-3-phenylpropyl)-η^1-phosphetane}]PF_6 (11a−c). General Procedure. A mixture of the tethered arene phosphetane complex **10** (0.25 mmol), aniline (1 equiv), and $NaPF_6$ (1.3 equiv) in CH_2Cl_2 (5 mL) and methanol (10 mL) was stirred overnight at room temperature. The solvent was removed under vacuum from the reaction mixture, and the resulting orange residue was washed several times with hexane. Addition of 10 mL of CH_2Cl_2 was followed by filtration. Pure complex salts were precipitated as orange crystals by slow addition of *n*-hexane. With the exception of ^{31}P NMR, the spectroscopic data are given for the major R_{Ru},S_C,S_C diastereomer; those of the second S_{Ru},S_C,S_C diastereomer fit to this interpretation.

[RuCl(aniline){2,4-dicylohexyl-1-(η^6-3-phenylpropyl)-η^1-phosphetane}]PF_6 (11a): yield 0.16 g, 87%; ^1H NMR (399.7 MHz, $CDCl_3$, δ) 7.75 (d, 2H, H_{ortho} $PhNH_2$), 7.41 (t, 2H, H_{meso} $PhNH_2$), 7.25 (t, 2H, H_{para} $PhNH_2$), 5.95 (t, 1H, η^6-C_6H_5), 5.54 (d, 1H, η^6-C_6H_5), 5.25 (t, 1H, η^6-C_6H_5), 5.02−5.00 (m, 1H, η^6-C_6H_5), 4.59 (t, 1H, η^6-C_6H_5), 4.24 (br, NH_2), 3.00−2.97 (m, 1H), 2.74−1.63 (m, 20H), 1.38−1.64 (m, 12H); $^{13}C\{^1H\}$ NMR (100.4 MHz, $CDCl_3$, δ) 147.89 (d, $J_{CP} = 3.3$ Hz, C_{ipso} $PhNH_2$), 130.03 ($PhNH_2$), 126.73 ($PhNH_2$), 120.74 ($PhNH_2$), 109.05 (m, C_{ipso} η^6-C_6H_5), 97.39 (d, $J_{CP} = 9.3$ Hz, η^6-C_6H_5), 95.50 (η^6-C_6H_5), 84.98 (η^6-C_6H_5), 82.19 (η^6-C_6H_5), 47.36 (d, $J_{CP} = 34.6$ Hz, CH), 38.66 (d, $J_{CP} = 5.7$ Hz, CH), 38.41 (CH), 37.91 (d, $J_{CP} = 21.4$ Hz, CH), 33.79 (d, superposed, $J_{CP} = 28.9$ Hz, CH_2), 32.35 (d, $J_{CP} = 16.6$ Hz, CH_2), 30.67 (d, $J_{CP} = 10.7$ Hz, CH_2), 28.15 (CH_2), 26.24−25.84 (m, superposed, CH_2), 20.81 (d, $J_{CP} = 14.1$ Hz, CH_2), 20.17 (CH_2); $^{31}P\{^1H\}$ NMR (161.7 MHz, $CDCl_3$, δ) 66.08 (94%), 58.22 (6%); mp 180 °C dec. Anal. Found (calcd) for $C_{30}H_{44}ClF_6P_2NRu$: C, 49.48 (49.28); H, 6.35 (6.07); N, 1.96 (1.92).

[RuCl(aniline){2,4-diisopropyl-1-(η^6-3-phenylpropyl)-η^1-phosphetane}]PF_6 (11b): yield 0.14 g, 88%; ^1H NMR (399.7 MHz, $CDCl_3$, δ) 7.72 (d, 2H, H_{ortho} $PhNH_2$), 7.38 (t, 2H, H_{meso} $PhNH_2$), 7.20 (d, 2H, H_{meso} $PhNH_2$), 5.92 (t, 1H, η^6-C_6H_5), 5.55 (d, 1H, η^6-C_6H_5), 5.28 (t, 1H, η^6-C_6H_5), 5.04−5.01 (m, 1H, η^6-C_6H_5), 4.61 (t, 1H, η^6-C_6H_5), 4.24 (br, NH_2), 2.75−1.85 (m, 12H, CH + CH_2), 0.99−0.88 (md, 12H, CH_3); $^{13}C\{^1H\}$ NMR (100.4 MHz, $CDCl_3$, δ) 147.66 (C_{ipso}, $PhNH_2$), 129.88 ($PhNH_2$), 126.61 ($PhNH_2$); 120.57 ($PhNH_2$); 108.91 (d, $J_{CP} = 9.8$ Hz, η^6-C_6H_5); 97.30 (d, $J_{CP} = 14.9$ Hz, η^6-C_6H_5), 95.23 (η^6-C_6H_5), 84.70 (η^6-C_6H_5), 82.19 (η^6-C_6H_5), 49.11(d, $J_{CP} = 34.7$ Hz, CH), 38.43 (d, $J_{CP} = 34.7$ Hz, CH), 33.20 (d, $J_{CP} = 12.0$ Hz, CH_2), 29.09 (d, $J_{CP} = 9.9$ Hz, CH), 29.06 (d, $J_{CP} = 4.9$ Hz, CH), 27.93 (d, $J_{CP} = 1.7$ Hz, CH_2), 25.59 (CH_2), 23.20 (d, $J_{CP} = 5.0$ Hz, CH_3), 23.03 (d, $J_{CP} = 3.3$ Hz, CH_3), 20.82 (d, $J_{CP} = 18.3$ Hz, CH_2), 20.57 (d, $J_{CP} = 13.4$ Hz, CH_2), 20.09 (d, $J_{CP} = 9.8$ Hz, CH_3), 20.7 (CH_3); $^{31}P\{^1H\}$ NMR (161.7 MHz, $CDCl_3$, δ): 68.91 (8%), 67.44 (92%); mp 167 °C dec. Anal. Found (calcd) for $C_{24}H_{36}ClF_6P_2NRu$: C, 44.61 (44.28); H, 5.57 (5.58); N, 1.80 (2.15).

[RuCl(aniline){2,4-di-*tert*-butyl-1-(η^6-3-phenylpropyl)-η^1-phosphetane}]PF_6 (11c): yield 0.15 g, 86%; ^1H NMR (270.2 MHz,

$CDCl_3$, δ) 7.77 (d, 2H, H_{ortho} $PhNH_2$); 7.39 (t, 2H, H_{meso} $PhNH_2$), 7.23 (d, 2H, H_{meso} $PhNH_2$), 5.98 (t, 1H, η^6-C_6H_5), 5.53 (d, 1H, η^6-C_6H_5), 5.22−5.18 (m, 1H, η^6-C_6H_5), 5.12 (t, 1H, η^6-C_6H_5), 4.47 (t, 1H, η^6-C_6H_5), 4.25 (br, NH_2), 2.97−2.91 (m, 1H), 2.73−2.40 (m, 9H), 1.04 (d, 18H, CH_3); $^{13}C\{^1H\}$ NMR (100.4 MHz, $CDCl_3$, δ) 147.72 (C_{ipso}, $PhNH_2$), 129.84 ($PhNH_2$), 126.75 ($PhNH_2$), 120.56 ($PhNH_2$), 106.61−106.44 (m, η^6-C_6H_5), 99.62−99.63 (m, η^6-C_6H_5), 83.80 (η^6-C_6H_5), 81.57 (η^6-C_6H_5), 78.23 (η^6-C_6H_5), 57.26(d, J_{CP} = 29.7 Hz, CH), 44.68 (d, J_{CP} = 19.8 Hz, CH), 33.45 (d, J_{CP} = 6.0 Hz, $C(CH_3)$), 32.86 (d, J_{CP} = 2.0 Hz, $C(CH_3)$), 29.82 (d, J_{CP} = 10.7 Hz, CH_2), 29.07 (superposed, CH_3), 28.87 (superposed, CH_3), 27.74 (CH_2), 24.79 (d, J_{CP} = 9.9 Hz, CH_2), 20.58 (CH_2); $^{31}P\{^1H\}$ NMR (161.7 MHz, $CDCl_3$, δ) 65.82 (93%), 60.60 (7%); mp 150 °C dec. Anal. Found (calcd) for $C_{26.5}H_{41}Cl_2F_6P_2NRu$: C, 43.99 (44.11); H, 6.45 (5.72); N, 1.85 (1.94).

Crystal Structure Determination of 5c, 6a,d, and 11a−c. Suitable single crystals were embedded in protective perfluoropolyether oil; data were collected at a temperature of 100 K on a Bruker-Nonius Kappa CCD diffractometer using Mo Kα radiation (λ = 0.710 73 Å, graphite monochromator). Data were corrected for Lorentz and polarization effects. Absorption effects have been taken into account using either a semiempirical correction based on multiple scans (**5c**, **6b**, **11a**,**b**[42]) or a numerical correction from indexing of crystal faces (**11c**[43]). For **6a** absorption effects have been neglected. Structures were solved by direct methods and refined by full-matrix least-squares procedures against F^2 with all reflections (SHELXTL 6.12[44]). All non-hydrogen atoms were refined anisotropically. The hydrogen atoms were geometrically positioned and allowed to ride on their carrier atoms during refinement; their isotropic displacement parameters were tied to those of the adjacent C, N, or B atoms by a factor of 1.2 or 1.5. Further remarks: the unit cells of **11b**,**c** contain two independent molecules in their asymmetric units. These independent molecules represent identical enantiomers with only slight differences of their conformations. Compound **11c** crystallizes with 0.5 CH_2Cl_2 per formula unit. This solvent molecule is disordered; two alternative positions have been refined to give site occupancies of 81.5(4) and 18.5(4)%, respectively. Similarity restraints have been applied in the refinement of the carbon atoms of the complex molecules (SIMU) and the disordered CH_2Cl_2 molecule (SAME, SIMU) of **11c**.

Acknowledgment. We thank the *Deutsche Forschungsgemeinschaft* (SFB 583) and the *Fonds der Chemischen Industrie* for generous financial support.

Supporting Information Available: CIF files giving crystallographic data for compounds **5c**, **6a**,**d**, and **11a−c**. This material is available free of charge via the Internet at http://pubs.acs.org.

OM050461Z

(42) SADABS 2.06; Bruker AXS, Inc., Madison, WI, 2002.

(43) Coppens, P. In *Crystallographic Computing*; Ahmed, F. R., Hall, S. R., Huber, C. P., Eds.; Munksgaard: Copenhagen, 1970; p 255.

(44) SHELXTL NT 6.12; Bruker AXS, Inc., Madison, WI, 2002.